Supporting Information:

Mechanism and kinetics of the electrocatalytic reaction responsible for the high cost of hydrogen fuel cells: guidelines for dramatic improvements.

Authors: Tao Cheng[1], William A Goddard III[1*], Qi An[1], Hai Xiao[1], Boris Merinov[1] and Sergey Morozov[2]

Affiliations:

[1]Materials and Process Simulation Center (MC139-74), California Institute of Technology, Pasadena, California 91125, United States.

[2]South Ural State University Lenina, 76, Chelyabinsk, Chelyabinsk Oblast, Russia Each

*Correspondence to wag@wag.caltech.edu

S1. Simulation Methods

Electronic structure calculations were performed within the framework of DFT, as implemented in the Vienna ab initio simulation program (VASP),[1-4] a plane-wave pseudopotential package. The exchange and correlation energies were calculated using the Perdew, Burke, and Ernzerhof (PBE) functional within the generalized gradient approximation (GGA). [5, 6] The PBE-D3 method was employed to correct van der Waals interaction of water-water and water-Pt.[7]

Our Calculations used a 3-layer Pt(111) metal slab, based on a 4 × 4 periodic cell with the bottom two layers fixed. The water slab contains 48 water molecules placed on the Pt(111) surface to simulate the water/Cu(111) interface explicitly. The thickness of the water slab is ~15 Å, corresponding to 5 layers of water. The simulation box is 50 Å along the z-axis with a vacuum of 30 Å. The lateral dimensions of the slab were fixed using the experiment lattice constant of 3.615 Å. A plane-wave cutoff energy of 400 eV was used. The First order Methfessel-Paxton scheme was used with a smearing width of 0.2 eV. Dipole corrections were applied along the z axis. The Energy minimization criterion was that forces on free atoms are < 0.01 eV/Å. The charges on species were derived using a Bader analysis.[8, 9]

A 1.2 fs time step with utilized in the QM-based Reactive Molecular Dynamics (RMD) simulations with the hydrogen mass set to 2 amu. These RMD simulations used only the gamma point of the Brillouin zone with no consideration of symmetry. The velocities were rescaled every 20 MD steps to readjust to the target temperature to equilibrium. We employed a Nose-Hoover thermostat for the free energy calculations with a temperature damping parameter of 100 fs.

To initialize the positions of the solvent atoms, we carried out ReaxFF RMD calculations at 298K for 2ns.[10] Then we minimized the final structure with QM, re-initialized the velocities at 50K, heated to 298K over five ps and then metadynamics for 2 to 10 ps.

S2. Metadynamics

The metadynamics Hamiltonian $\tilde{H}(p,q,t)$ is written as:[11]

$$\tilde{H}(p,q,t) = H(p,q) + \tilde{V}(t,\xi), \quad \text{(S1)}$$

where *H(p,q)* is the Hamiltonian for the original (unbiased) system, ξ is the collective variable (**CV**), and $\tilde{V}(t,\xi)$ is the time-dependent bias potential. The bias term is defined as a sum of Gaussian hills with **height *h*** and **width *ω***:

$$\tilde{V}(t,\xi) = h\sum_{i=1}^{|t/t_G|} \exp[-\frac{|\xi^{(t)}-\xi^{(i\cdot t_G)}|^2}{2\omega}], \quad \text{(S2)}$$

The biased potential is related to the free energy via:

$$A(\xi) = \lim_{t\to\infty} \tilde{V}(t,\xi) + const \quad \text{(S3)}$$

In this work we used:

- h = 0.08 eV
- ω = 0.18 Å
- t_G = 20 time step

S3. Constrained Molecular dynamics[12]

The correct (*unbiased*) average for a quantity $\alpha(\xi)$ of constrained (*biased*) molecular dynamics can be obtained from:

$$\alpha(\xi) = \frac{\left\langle |\boldsymbol{Z}|^{-\frac{1}{2}}\alpha(\xi^*)\right\rangle_{\xi^*}}{\left\langle |\boldsymbol{Z}|^{-\frac{1}{2}}\right\rangle_{\xi^*}} \quad \text{(S4)}$$

where Z is a mass metric tensor defined as:

$$\boldsymbol{Z}_{\alpha,\beta} = \sum_{i=1}^{3N} m_i^{-1}\nabla_i\xi_\alpha \cdot \nabla_i\xi_\beta \quad \text{(S5)}$$

the free energy gradient can be computed using the equation:

$$\left(\frac{\partial A}{\partial \xi_k}\right)_{\xi^*} = \frac{1}{\left\langle |\boldsymbol{Z}|^{-\frac{1}{2}}\right\rangle_{\xi^*}}\left\langle |\boldsymbol{Z}|^{-\frac{1}{2}}\left[\lambda_k + \frac{k_B T}{2|\boldsymbol{Z}|}\sum_{j=1}^{r}(\boldsymbol{Z}^{-1})_{kj}\sum_{i=1}^{3N} m_i^{-1}\nabla_i\xi_j \cdot \nabla_i|\boldsymbol{Z}|\right]\right\rangle_{\xi^*} \quad \text{(S6)}$$

The free-energy difference between states (1) and (2) was computed by integrating the free-energy gradients over a connecting path:

$$\Delta A_{1\to 2} = \int_{\xi(1)}^{\xi(2)} \left(\frac{\partial A}{\partial \xi}\right)_{\xi} \cdot d\xi \quad \text{(S7)}$$

First, we employed slow-growth to generate the reaction path. Then we applied an increment of 0.0008 Å/step in the collective variables to drive the chemical reactions. We found that simulation times of 2 to 10 ps were necessary to complete the reaction, depending on the length of reaction pathways. From the reactive trajectories, we selected 20 windows (21 points) for thermodynamic integration calculations. Simulations of 2.4 ps were carried out at each window to produce the potential of mean force (PMF). Energy profiles were obtained by integrating the PMF.

S4. Reactive trajectories and free energy contours

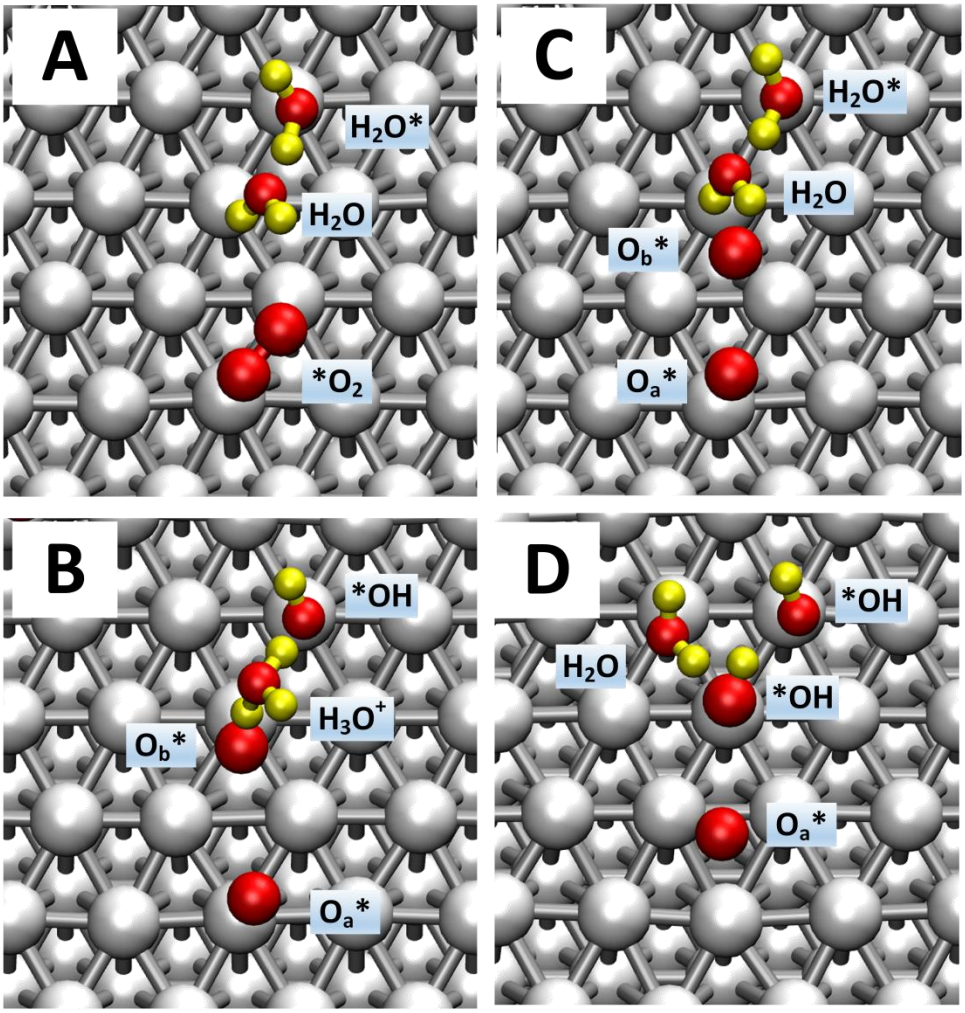

Fig. S1. Snap shots from the QM RμD trajectories showing the dissociation of O_2 (reaction 1a, $O_2^* \rightarrow 2 \cdot O^*$, with $\Delta G^{\ddagger}$ = 0.40 eV) followed by O* hydration (reaction 2c, $O^* + H_2O^* \xrightarrow{H_2O(aq)} {}^*OH + {}^*OH$ with $\Delta G^{\ddagger}$ = 0.25 eV).

(a) t = 0 ps. O_2 on the bridge site;

(b) t = 0.43 ps. O_a^* on top site and O_b^* on HCP site

(c) t = 0.48 ps. intermediate state of O_b^* hydration

(d) t = 0.78 ps. O_a^* on FCC site, and the newly formed *OH on top site.

The colors of atoms are Pt in silver, H in yellow (for viewing convenience), and O in red.

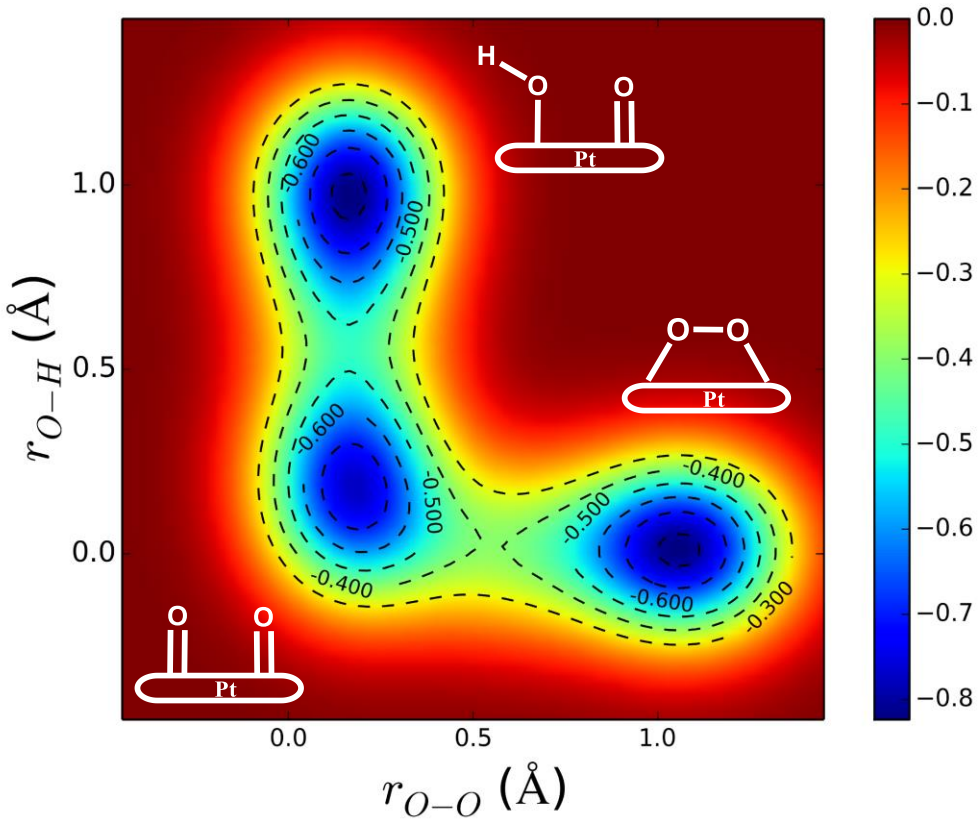

Fig. S2. Two-dimensional free energy contours for QM RμD of O_2 dissociation ($^*O_2 \longrightarrow O^* + O^*$, $\Delta G^{\ddagger}$ = 0.40 eV) along with oxygen hydration by surface water ($O^* + H_2O^* \xrightarrow{H_2O(aq)} {}^*OH + {}^*OH$, $\Delta G^{\ddagger}$ = 0.25 eV). The two collective variables are the O-O distance ($r_{O\text{-}O}$) and O-H distance ($r_{O\text{-}H}$). We conclude that there is no concerted coupling, however, in the dynamics, the system goes over the second barrier in 0.30 ps, suggested that the energy released from the first step promotes the second step.

To determine if this 2c O* hydrolysis aids the decomposition of O_2 in step 1a, we carried out a two-dimensional free energy calculation by extending the CV to two dimensions with one being the coordination number of O [N(O)] and the other the coordination number of H [N(H)] (taking the central O as reference). The calculated 2D free energy surface is shown in Fig. S2. There is essentially no correlation between the two CVs, indicating that these reactions are two separate events. O_2 decomposition (1a) has a higher energy barrier of 0.40 eV, while O* hydration (2c) has a lower energy barrier, 0.25 eV. This second hydrolysis step was observed during the timescale of the O_2 dissociation, suggesting that some of the reaction energy of the 1st step is used to drive the second step, rather than being dissipated.

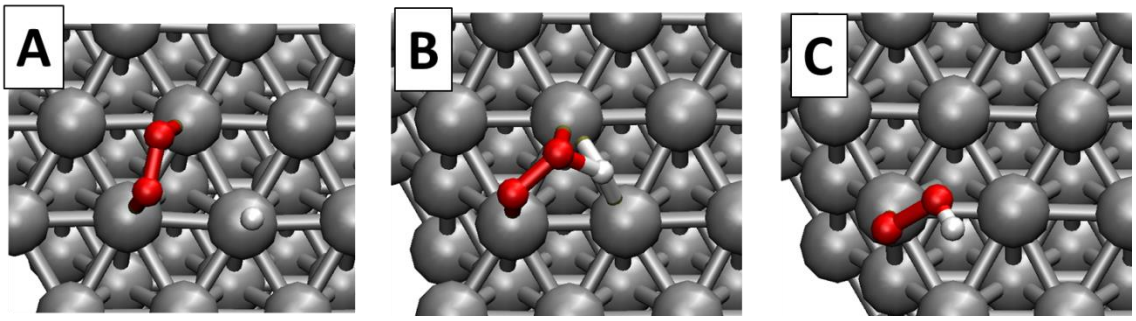

Fig. S3. Reactive trajectories from QM RμD showing the *OOH formation from H*, reaction 1b

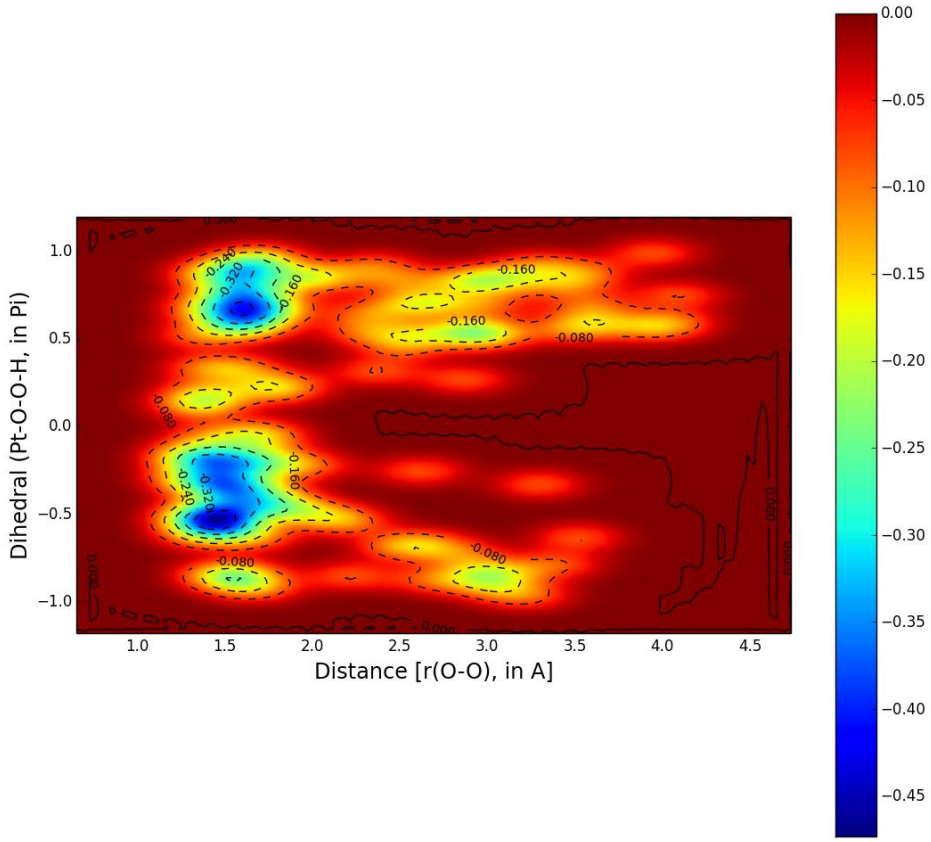

Fig. S4. Two-dimensional free energy contours for *OOH dissociation. The two collective variables (CVs) are O-O distance [r(O-O)] and the dihedral angle of Pt-O-O-H. The predicted free energy barrier is $\Delta G^{\ddagger} =$ 0.38 eV, which is $\Delta G^{\ddagger} = 0.32$ eV lower than that derived by using only one CV, which demonstrates that selecting the CV properly is essential for complex reactions.

Assuming the O-O distance as the CV for *OOH decomposition, we found a 0.70 eV dissociation energy barrier for *OOH direct decomposition (1b). This is unreasonable since the direct O_2 decomposition has an energy barrier of 0.40 eV. In examining these reactions, we found that the Pt-O-O-H dihedral angle rotates significantly during the reaction trajectories. Therefore, we extended the CV to be two-dimensional including the dihedral angle of Pt-O-O-H as a 2nd CV. This 2D metadynamics simulation decreases free energy barrier to 0.38 eV, leading to the 2D free energy contours shown in Fig S4. These results demonstrate that selecting the CV properly is essential for complex reactions.

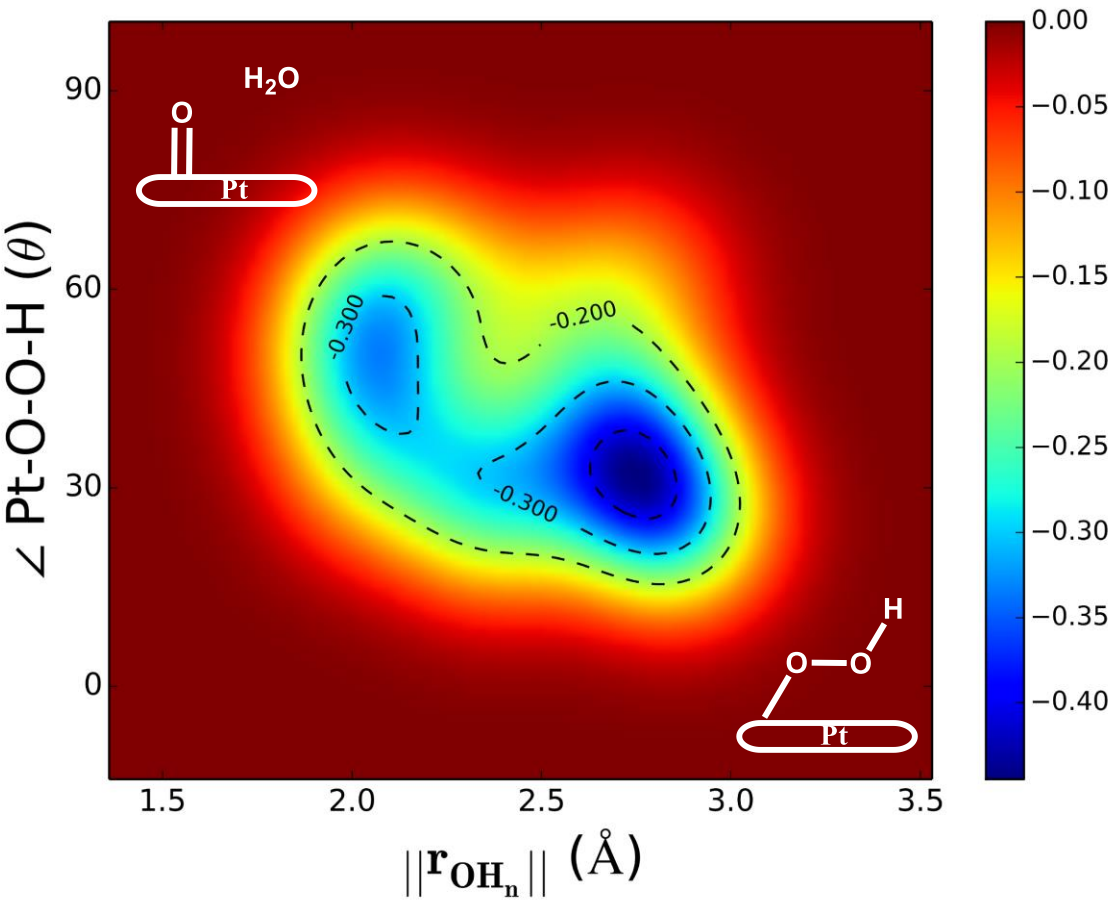

Fig. S5. Two-dimensional free energy contours for HOO* reduction. The two collective variables (CVs) are Norm of HB chains $||r_{OHn}||$ and a dihedral angle of Pt-O-O-H. The predicted free energy barrier is 0.14 eV.

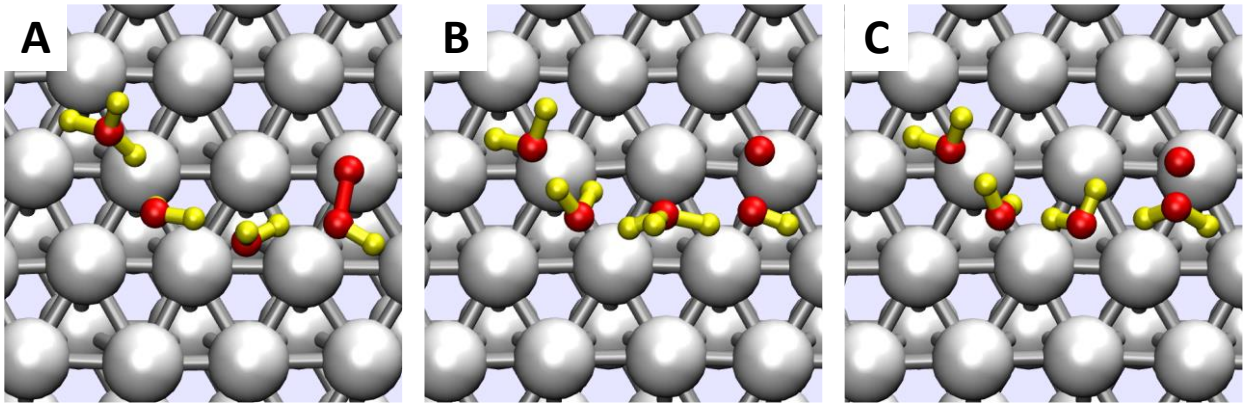

Fig. S6. Reactive trajectories from meta-dynamics showing the *OOH reduction (reaction 1c') via an ER mechanism. This leads to a free energy barrier of 0.14 eV at U=0.6 V

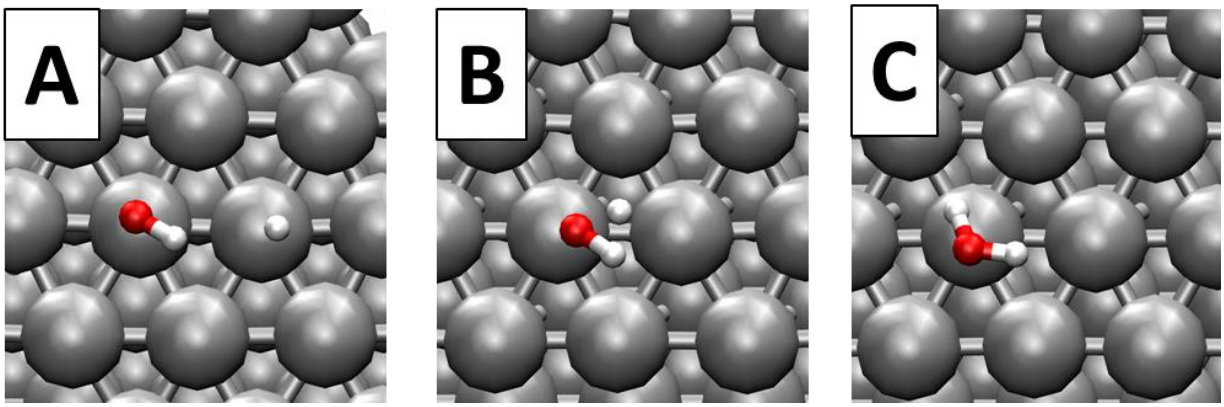

Fig. S7. Reactive trajectories from meta-dynamics showing the water formation (LH) from OH* +H* with a free energy barrier of 0.54±0.08 eV (reaction 3a). For comparison, we also carried out a simulation with a 4-layer slab with the bottom two layers fixed for this reaction of the water formation (LH) from OH* +H*. For comparison, we also carried out a simulation with a 4-layer slab with the bottom two layers fixed for this reaction. The free energy barrier obtained from this 4-layer slab is 0.59 eV, which is consistent with that obtained from 3-layer slab calculation (0.54 eV) considering the errors in the calculation (0.08 eV). Therefore, the 3-layer models were used in this work for the sake of efficiency.

S5. Constant potential corrections

Electrochemical reaction energetics at constant potential were determined using the correction method proposed by Chan and Norskov:[13]

$$\Delta E_{\phi_1-\phi_2} = E(\phi_1) - E(\phi_2) = \frac{\Delta q \cdot \Delta \Phi}{2} \quad \text{(S8)}$$

However, for plane wave calculations the atomic charges are ambiguous. Instead, we use the capacitance (C) defined as:

$$C = \frac{\Delta q}{\Delta \phi} \quad \text{(S9)}$$

To replace change (q), in S8, which can be calculated by varying the number of total electrons. This leads to the ΔE in S10:

$$\Delta E = \frac{C \cdot \Delta \Phi^2}{2} \quad \text{(S10)}$$

The resultant extrapolated energy differences (ΔE) are shown in Table S1. These corrections were applied only to the proton transfer reactions.

Table S1. Corrections to obtain the free energy barriers at a constant potential. Tabulated work function, Φ (in V), C (in e/V), and the extrapolated ΔE (in eV) at Φ_{t0}.

Step	Reactions	Φ (V)		C(e/V)	ΔE(eV)
		t_0	t_{TS}		
1a	O_2* dissociation	5.3(4)	5.2(6)	2.0	0.02
1b''	HOO* reduction	4.8(6)	4.7(3)	1.8	0.03
1b'''	HOOH formation	4.3(7)	4.4(4)	2.1	-0.01
2a	O* hydration	5.3(4)	5.3(5)	1.9	0.00
3a	water formation	5.5(5)	5.4(4)	1.8	0.01
3b	Water formation (ER @ 0.6 V)	5.0(7)	5.2 (6)	1.8	-0.04
3b	Water formation (ER @ 1.1 V)	5.5(4)	5.7(5)	2.1	-0.04

References and Notes

1. G. Kresse and J. Hafner, *Phys. Rev. B: Condens. Matter Mater. Phys.*, 1993, **47**, 558-561.
2. G. Kresse and J. Hafner, *Phys. Rev. B: Condens. Matter Mater. Phys.*, 1994, **49**, 14251-14269.
3. G. Kresse and J. Furthmüller, *Comput. Mater. Sci.*, 1996, **6**, 15-50.
4. G. Kresse and J. Furthmüller, *Phys. Rev. B: Condens. Matter Mater. Phys.*, 1996, **54**, 11169-11186.
5. J. P. Perdew, J. A. Chevary, S. H. Vosko, K. A. Jackson, M. R. Pederson, D. J. Singh and C. Fiolhais, *Phys. Rev. B: Condens. Matter Mater. Phys.*, 1992, **46**, 6671-6687.
6. J. P. Perdew, J. A. Chevary, S. H. Vosko, K. A. Jackson, M. R. Pederson, D. J. Singh and C. Fiolhais, *Phys. Rev. B: Condens. Matter Mater. Phys.*, 1993, **48**, 4978-4978.
7. S. Grimme, J. Antony, S. Ehrlich and H. Krieg, *J. Chem. Phys.*, 2010, **132**, 154104.
8. R. F. W. Bader, *Chem. Rev.*, 1991, **91**, 893-928.
9. G. Henkelman, A. Arnaldsson and H. Jónsson, *Comput. Mater. Sci.*, 2006, **36**, 354-360.
10. J. Ludwig, D. G. Vlachos, A. C. T. van Duin and W. A. Goddard, *J. Phys. Chem. B*, 2006, **110**, 4274-4282.
11. A. Laio and M. Parrinello, *Proc. Natl. Acad. Sci. U. S. A.*, 2002, **99**, 12562-12566.
12. P. Fleurat-Lessard and T. Ziegler, *J. Chem. Phys.*, 2005, **123**, 084101.
13. K. Chan and J. K. Nørskov, *J. Phys. Chem. Lett.*, 2016, **7**, 1686-1690.